Structural Characterization of Binding of Cu(II) to Tau Protein[†]

Alice Soragni,[‡,§] Barbara Zambelli,[§] Marco D. Mukrasch,[‡] Jacek Biernat,[||] Sadasivam Jeganathan,[||] Christian Griesinger,[‡] Stefano Ciurli,[§,⊥] Eckhard Mandelkow,[||] and Markus Zweckstetter*[,‡,#]

Department for NMR-Based Structural Biology, Max Planck Institute for Biophysical Chemistry, Am Fassberg 11, 37077 Göttingen, Germany, Laboratory of Bioinorganic Chemistry, Department of Agro-Environmental Science and Technology, University of Bologna, Viale Giuseppe Fanin 40, 40127 Bologna, Italy, Max Planck Unit for Structural Molecular Biology, c/o DESY, Hamburg, Germany, CERM, Center for Magnetic Resonance, Firenze, Italy, and DFG Research Center for the Molecular Physiology of the Brain, Göttingen, Germany

Received May 13, 2008; Revised Manuscript Received August 19, 2008

ABSTRACT: Transition metals have been frequently recognized as risk factors in neurodegenerative disorders, and brain lesions associated with Alzheimer's disease are rich in Fe(III), Zn(II), and Cu(II). By using different biophysical techniques (nuclear magnetic resonance, circular dichroism, light scattering, and microcalorimetry), we have structurally characterized the binding of Cu(II) to a 198 amino acid fragment of the protein Tau that can mimic both the aggregation behavior and microtubule binding properties of the full-length protein. We demonstrate that Tau can specifically bind one Cu(II) ion per monomer with a dissociation constant in the micromolar range, an affinity comparable to the binding of Cu(II) to other proteins involved in neurodegenerative diseases. NMR spectroscopy showed that two short stretches of residues, ^{287}VQSKCGS^{293} and ^{310}YKPVDLSKVTSKCGS^{324}, are primarily involved in copper binding, in agreement with mutational analysis. According to circular dichroism and NMR spectroscopy, Tau remains largely disordered upon binding to Cu(II), although a limited amount of aggregation is induced.

It has been recently estimated that 24.3 million people are suffering from dementia worldwide (*1*), and Alzheimer's disease (AD[1]) accounts for the majority of the cases (70% for individuals over the age of 65) (*2*). Aging is the major risk factor for AD (*3*), whereas in the past few years other elements have been linked to the disease, such as oxidative damage and heavy metals (*4*). Among metals, copper plays a pivotal role. Proteins directly linked to AD, such as amyloid precursor protein (APP) and amyloid-β peptide (Aβ), are involved in copper trafficking and homeostasis, which is impaired in case of disease (*5, 6*). Moreover, the concentration of copper and other metals increases with aging in several tissues, including the brain. Copper is found at high concentration (0.4 mM) in amyloid plaques (*7*) and the presence of transition metals in neurofibrillary tangles (NFT) has been reported (*8*). Although the free cytosolic copper concentration is supposed to be very low (*9*), a redistribution of copper among different compartments and a defective metal homeostasis could result in an increased copper availability. Moreover, it has been demonstrated that metal driven cellular redox activity takes place in the cytosol (*10*). Importantly, ion metals such as Cu(II) promote the pathogenic aggregation of several proteins involved in neurodegenerative diseases like Aβ, α-synuclein, and prion protein, by direct binding to these polypeptides with micromolar dissociation constants (*11*−*13*).

Tau is a microtubule (MT) binding protein that interacts with tubulin to trigger MT formation and stabilization, neurite outgrowth and other MT-dependent functions (*14*). The stability of MT can be altered by the state of Tau, such as its phosphorylation, isoform composition, and other modifications (*15*). Aggregation of Tau and formation of neurofibrillary tangles, constituted of paired helical filaments (PHF), is one of the characteristic traits of Alzheimer's disease. The tangles are found in the amygdala, hippocampus, entorhinal cortex, association cortex and sensory cortex (*16*). Tau exists in six different isoforms in the human brain, ranging from 352 to 441 residues. All isoforms contain a repeat domain in the C-terminal half, which consists of three to four pseudorepeat sequences (∼31 residues each). The second and third repeats contain two hexapeptide motifs (^{275}VQIINK^{280} and ^{306}VQIVYK^{311}), that are essential for aggregation of Tau into paired helical filaments (PHFs) (*17*).

Tau belongs to the class of intrinsically disordered proteins with no apparent ordered secondary structure detectable by circular dichroism or infrared spectroscopy (*18*). Disordered

[†] B.Z. is a recipient of a joint fellowship from the University of Bologna and CERM/CIRMMP (Firenze). This work was supported by the Max Planck Society, the Fonds der Chemischen Industrie, the Boehringer Ingelheim Fonds (GRK 782) and through a DFG Heisenberg scholarship to M.Z. (ZW 71/2-1 and 3-1).

* To whom the correspondence should be addressed. Tel: +49 551 201 2220. Fax: +49 551 201 2202. E-mail: mzwecks@gwdg.de.

[‡] Max Planck Institute for Biophysical Chemistry.

[§] University of Bologna.

[||] Max Planck Unit for Structural Molecular Biology.

[⊥] CERM, Center for Magnetic Resonance.

[#] DFG Research Center for the Molecular Physiology of the Brain.

[1] Abbreviations: 2D, two-dimensional; AD, Alzheimer's disease; Aβ, amyloid beta; CD, circular dichroism; CT-HNCA, constant time HNCA; DLS, dynamic light scattering; DOSY, diffusion ordered spectroscopy; DTNB, 5,5′-dithio-bis(2-nitrobenzoic acid); DTT, dithiothreitol; EDTA, ethylenediaminetetraacetic acid; HSQC, heteronuclear single quantum coherence; ICP-ES, inductively coupled plasma emission spectroscopy; ITC, isothermal titration calorimetry; IUP, intrinsically unfolded protein; MES, 2-(*N*-morpholino)ethanesulfonic acid; MT, microtubules; NMR, nuclear magnetic resonance; PHF, paired helical filaments; SEC-MALS, multiangle light scattering coupled to size exclusion chromatography.

10.1021/bi8008856 CCC: $40.75
Published on Web 09/20/2008

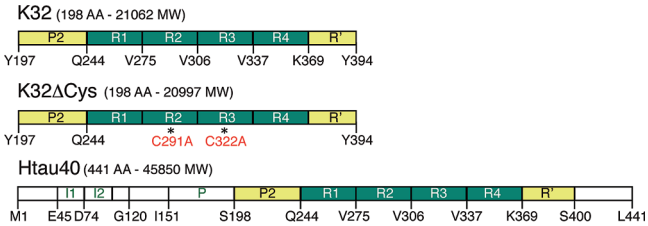

FIGURE 1: Tau isoform and Tau-derived constructs. Domain organization of Tau fragments K32 and K32ΔCys and of Htau40, the largest isoform present in the human central nervous system (441 residues). Six isoforms are produced by alternative splicing. The C-terminal half-contains three or four pseudorepeats (31 residues each ca., R1−R4, green boxes), which are involved in MT binding and form the core of PHFs. In the mutant K32ΔCys, the two cysteines were replaced by alanines. Residue numbers label domain boundaries.

proteins are not amenable for crystallography, and NMR spectroscopy is the only method that allows a description of their conformations and interactions with high resolution (*19*). The lack of an ordered structure, however, causes dramatic signal overlap, limiting quantitative NMR studies to nonglobular proteins with less than 200 amino acids. Recently, we have determined the backbone assignment of a 198 amino acid fragment (K32) of Tau, determined its residual secondary structure and characterized its interaction with MTs and the aggregation inducer heparin (*20*). K32 comprises the repeat domain as well as the two flanking regions (Figure 1) and mimics the aggregation behavior and MT-binding properties of the full-length protein (*20*).

Several biophysical and structural studies have revealed detailed insights into the interaction of Cu(II) with Aβ, α-synuclein, prion protein and amyloid precursor protein (*11*−*13, 21*). Much less is known about the interaction of transition metals with Tau. Previous studies suggested that metals such as aluminum and iron(III) can promote the *in vitro* aggregation of hyperphosphorylated Tau (*22, 23*). Moreover, direct binding of Cu(II) to short peptides comprising either the first, second or the third repeat of Tau was demonstrated (*24*−*26*). The molecular details of Cu(II) binding to full-length Tau, however, are an open question. In particular, it is unclear whether the first, second or third repeat binds Cu(II) in Tau isoforms that contain all of them, whether these are the only binding sites, and what are the structural consequences of binding of Cu(II) to Tau.

Here we report a study of the binding of Cu(II) to Htau40, the longest Tau isoform found in the human brain, and, at higher resolution, to the 198-residue Tau fragment K32. The studies were performed in oxidative conditions at pH 6.5, mimicking the environment present during inflammation (*27*). In order to probe the importance of cysteines for the interaction with Cu(II), we designed a mutant protein, in which the two natively occurring Cys291 and Cys322 were mutated into alanine. Our studies demonstrate that Tau can specifically bind one Cu(II) ion per monomer with dissociation constants in the micromolar range, comparable to the binding affinity of Cu(II) to other unfolded proteins involved in neurodegenerative diseases.

EXPERIMENTAL PROCEDURES

Expression, Isotopic Labeling and Purification of Recombinant Tau Constructs. Human Tau40 isoform (441 aa), K32 comprising residues (Met)Ser198−Tyr394, equivalent to the four repeats and the two flanking regions (198 residues), and K32Δcys with Cys291, and Cys322 replaced by Ala residues were expressed and purified as described (*20, 28*). Briefly, the expressed proteins were purified from bacterial extracts by making use of the heat stability of the protein and by FPLC SP-Sepharose chromatography (GE Healthcare, Freiburg, Germany). To label the Htau40 protein with ^{15}N and ^{13}C isotopes, the *Escherichia coli* culture was grown in an M9 minimal medium with $^{15}NH_4Cl$ (1 g/L) and ^{13}C glucose (4 g/L) (Euriso-Top, Germany).

To label the K32 and K32Δcys proteins with ^{15}N stable isotope, the *E. coli* cultures expressing these proteins were grown in a M9 minimal medium with $^{15}NH_4Cl$ (1 g/L) (Euriso-Top, Germany). *E. coli* cultures expressing double labeled K32 and K32Δcys proteins were grown on rich growth medium based on chemolithoautotrophic bacteria labeled with ^{15}N and ^{13}C isotopes (Silantes, Munich, Germany). The *E. coli* protein extracts were dialyzed against the exchange chromatography buffer A (20 mM MES, 50 mM NaCl, 1 mM EGTA, 1 mM $MgCl_2$, 2 mM DTT, 0.1 mM PMSF, pH 6.8) and loaded on FPLC SP-Sepharose column. The proteins were eluted by a linear gradient of cation exchange chromatography buffer B (20 mM MES, 1 M NaCl, 1 mM EGTA, 1 mM $MgCl_2$, 2 mM DTT, 0.1 mM PMSF, pH 6.8). In the second purification step, the breakdown products of Tau were removed by gel filtration using Superdex G75 with PBS buffer (137 mM NaCl, 3 mM KCI, 10 mM Na_2HPO_4, 2 mM KH_2PO_4, pH 7.4 with 1 mM DTT).

NMR Sample Preparation. NMR samples were freshly dialyzed into buffer before usage. After 3 to 4 h dialysis, samples were filtered using Ultrafree-MC tubes (0.22 μm centrifuge filters, Millipore) for 4 min at 12000*g*. Prior to usage, filters were washed for 2 min at 12000*g* using dialysis buffer. NMR samples contained 0.08−0.2 mM ^{15}N- or $^{15}N/^{13}C$-labeled protein in 90% H_2O, 10% D_2O, 20 mM MES, pH 6.5, NaCl 100 mM and no DTT in order to study Cu(II) binding.

NMR Spectroscopy. NMR spectra were acquired at 278 K on Bruker DRX 800, Avance 700, and 900 MHz NMR spectrometers. Aggregation did not occur at this temperature. The $^1H-^{15}N$ HSQC spectrum consisted of 8 scans, spectral windows of 12 ppm in the proton and 25 ppm in the nitrogen dimension. For backbone resonance assignment, a 3D CT-HNCA (*29*) was used. The spectrum (4 scans) was acquired with 2k complex points in t_3, 80 increments in t_2 (^{15}N dimension with echo−antiecho selection) and 156 increments in t_1 (^{13}C dimension with States-TPPI detection). Spectral widths in ppm were 10 (^1H), 24 (^{15}N), and 24 (^{13}C). ^1H chemical shifts were referenced to external DSS (2,2 dimethyl-2-silapentane-5-sulfonate), and indirectly for ^{15}N and ^{13}C (*30*). All data have been processed using NMRPipe (*31*) and analyzed using the software Sparky (*32*).

To determine the diffusion coefficient of the protein in solution, 2D diffusion-ordered spectroscopy (DOSY) (*33*) was performed at 300 K. A series of spin echo spectra were measured with increasing pulsed field gradient strengths (128 scans, 16 spectra, gradient from 2% to 95%). Signal decays of the methyl region were fitted to a single exponential decay in order to extract the diffusion coefficients (D_τ). From the diffusion coefficient the hydrodynamic radius was calculated according to

$$R_h = \frac{k_b T}{6\pi\eta D_\tau}$$

where k_b is the Boltzmann constant, T is the absolute temperature and η is the solvent viscosity.

The predicted hydrodynamic radius value was calculated according to the formula (*33*)

$$R_h = 2.21N^{0.57}$$

where R_h is the hydrodynamic radius in angstroms and N the number of residues.

Cu(II)−protein titrations were performed on uniformly ^{15}N-labeled samples containing 100−200 μM K32 or K32Δcys in MES buffer 20 mM, pH 6.5, 100 mM NaCl. Copper sulfate ($CuSO_4$, AppliChem) was used for the titration assays, which were monitored recording 2D ^{1}H−^{15}N HSQCs. Spectra were recorded for each step upon addition of increasing copper concentration. Complex formation was monitored at 278 K for ratios (Cu(II):protein) of 0.006, 0.013, 0.02, 0.03, 0.05, 0.2 and 0.4. Amide backbone cross peaks affected during the titration were characterized through chemical shift perturbation analysis. The mean chemical shift difference Δ_{av} normalized and weighted for each amino acid was calculated as

$$\Delta_{av} = \sqrt{\frac{(\Delta_{NH})^2 + (\Delta_N/5)^2}{2}}$$

where Δ_i is the difference between the free and bound state.

The electron spin relaxation from the paramagnetic Cu(II) results in differential broadening of amide resonances linked to the paramagnetic center (*12*). Intensity profiles for the cross peaks were obtained by plotting the I/I_0 ratio as a function of the protein sequence, where I_0 is the intensity of the peak in the absence of Cu(II) and I is the same peak intensity with copper. The spectra were then corrected taking into consideration the stepwise increase in sample volume.

Secondary chemical shift values were calculated as the differences between the measured Cα chemical shifts and the empirical random coil value of the appropriate amino acid type at pH 2.3 and 293 K in 8 M urea (*30*). Random coil values for histidines, glutamates, and aspartates were taken from Wishart (*31*), as the chemical shifts of these amino acids are particularly sensitive to pH, and the pH in the studies by Wishart (pH 5.0) is similar to the value used in this study (pH 6.5). Values for residues that are followed by a proline were also corrected (*32*).

Circular Dichroism. The CD spectra of K32 and K32Δcys have been recorded using a Chirascan (AppliedPhotophysics) spectropolarimeter flushed with nitrogen and equipped with a PCM.4 four position sample changer with Peltier temperature control in ammonium acetate buffer, which combine a low absorption rate to a high copper solubility. The experiments have been carried out incubating the protein of interest at room temperature (concentration 100−150 μM) and then diluting the sample to a final concentration of 8 μM. All samples were filtered through a 0.2 μm filter prior to use to remove dust and other particles that can interfere with the measurements.

CD profiles were registered at room temperature in the range 190−250 at 0.5 nm step for the far-UV. Eight spectra were accumulated to get proper signal-to-noise ratio. The secondary structure composition of the samples was evaluated at the Dichroweb server of the Centre for Protein and Membrane Structure and Dynamics (*35*) using the programs CDSSTR, SELCON3 and ContinLL and the reference sets 7. The best solution from the three algorithms was averaged.

Multiangle Light Scattering. The protein (100 μL, 1 mg/mL) in 20 mM MES (pH 6.5), 100 mM NaCl was loaded onto a Superdex-75 HR10/30 column (Amersham), pre-equilibrated with the same buffer, and eluted at room temperature at a flow rate of 0.5 mL/min. The molar mass and the hydrodynamic radius of K32 and K32Δcys in native condition, in the absence or presence of copper (1 mM) were determined using a combination of size-exclusion chromatography, connected downstream to a multiple-angle laser light (690.0 nm) scattering DAWN EOS photometer (Wyatt Technology). Values of 0.185 for the refractive index increment (dn/dc) and 1.330 for the solvent refractive index were used. Molecular weights were determined from a Zimm plot. Data were analyzed using Astra version 5.1.7 (Wyatt Technology), following the manufacturer's instructions.

Dynamic Light Scattering. The protein (100−150 μM, 50 μL) was measured at the desired temperature (5 or 25 °C) using a Zetasizer Nano ZS (Malvern) operating at a wavelength of 633 nm.

Calorimetric Measurements. Titration experiments were performed at 25 °C using a high-sensitivity VP-ITC microcalorimeter (MicroCal LLC, Northampton, MA). In each experiment, 30 injections (10 μL) of a solution containing $CuSO_4$ at a concentration of 400 μM were titrated into a solution of Htau40 (20 μM), K32 (22 μM) or K32ΔCys (30 μM) in the same buffer (cell volume = 1.4093 mL, stirring speed = 290 rpm) using a computer-controlled 310 μL microsyringe. The metal solution was prepared from a 0.5 M $CuSO_4$ stock diluting the Cu(II) in the buffer used to dialyze the protein just prior each experiment (20 mM MES, pH 6.5, 100 mM NaCl). The pH of each solution was checked before starting the analysis. The reference cell was filled with deionized water. Before each experiment, the protein solution was degassed for 2−5 min, to eliminate air bubbles, using the ThermoVac accessory of the microcalorimeter. The first addition started after the baseline stability was achieved. To allow the system to reach equilibrium, a spacing of 600 s between each ligand injection was applied. A control experiment was set up, titrating the copper solution into the buffer under the same conditions. Integrated heat data were fitted using a nonlinear least-squares minimization algorithm to a theoretical titration curve, using the MicroCal Origin software and a single set of binding sites model. In detail, for the binding of Cu(II) to the protein (Cu(II) + K32 ↔ K32·Cu(II)):

$$\frac{dQ}{d[Cu(II)]_t} = \Delta H^\circ V_o \left[\frac{1}{2} + \frac{1 - \left(\frac{[Cu(II)]_t}{[K32]_t}\right) - \left(\frac{K_d}{[K32]_t}\right)}{2\sqrt{\left[1 + \left(\frac{[Cu(II)]_t}{[K32]_t}\right) - \left(\frac{K_d}{[K32]_t}\right)\right] - 4\left(\frac{[Cu(II)]_t}{[K32]_t}\right)}} \right]$$

Ellman's Assay. The concentration of free sulfhydryl groups was determined using the Ellman's reagent DTNB (Sigma). Duplicates protein samples at a concentration of 180 μM were incubated for 10 min at room temperature in

presence of $CuSO_4$ in an equal molar concentration or 10-fold excess. Controls without copper were incubated in the same way. DTNB at a final concentration of 100 μM dissolved in Tris buffer and EDTA 1 mM was added to the samples and measured at 412 nm after 2 min in a Jasco spectrometer (Jasco V-650).

RESULTS

K32 and K32Δcys Are Metal-Free, Monomeric and Disordered in Solution. Three Tau constructs were used in this study (Figure 1): (i) Htau40, the longest Tau isoform found in the human brain, (ii) K32, comprising the four pseudorepeats involved in MT binding and fibrillization as well as the proline rich flanking regions on the two sides, and (iii) K32Δcys, a mutant in which the two cysteines (residues 291 and 322) were mutated into alanine. The purified proteins were checked for the presence of any metal bound, using inductively coupled plasma emission spectroscopy (ICP-ES), with a procedure previously described (*36*). Trace metals, comprising copper, were absent, confirming the metal-free state of the isolated proteins in the present conditions.

Size-exclusion chromatography equipped with multiangle light scattering detector (SEC-MALS) analysis of K32 (Figure S1 in the Supporting Information) and K32Δcys (data not shown) in their apo form showed a single protein peak and a homogeneous molar mass distribution. Thus, under the conditions studied, K32 is a monomer in solution, consistent with previous findings for Htau40 (*37*). In previous studies a reducing agent (dithiothreitol, DTT) was added in solution to avoid the formation of disulfide bridges (*20*). Light scattering and circular dichroism, however, showed that K32 did not undergo significant dimerization without DTT during the time scale of the experiments (data not shown). Moreover, since the radius of the protein remained constant, there was no substantial formation of disulfide bridges. This idea was further supported by the Ellman's assay, which showed no significant reduction in the concentration of free sulfhydryls during an incubation period of one hour (data not shown).

2D diffusion ordered spectroscopy estimated a radius of 4.5 ± 0.2 nm at a temperature of 25 °C (Figure 5B). For a fully unfolded protein of the same length, a hydrodynamic radius of 4.6 nm is expected (*33*). Two-dimensional NMR spectra further confirmed the disordered state of K32 and K32Δcys. $^1H-^{15}N$ heteronuclear single quantum correlation (HSQC) spectra of ^{15}N labeled K32 and K32Δcys mutant exhibited a limited dispersion of resonances (around 1 ppm) in the proton dimension (Figure 2A). In the HSQC of the mutant the cysteine peaks were no longer visible (Figure S2A in the Supporting Information). In addition, a number of small changes in the resonances of nearby residues were observed, reflecting the different chemical environment caused by the replacement of cysteines with alanines (Figure S2B in the Supporting Information).

Residual Secondary Structure of K32 in MES Buffer. Previously, the sequence-specific assignment of K32 resonances had been determined in phosphate buffer at pH 6.8 (*20*). To enable the characterization of K32:Cu(II) interaction, the resonance assignment of K32 was required in a buffer compatible with Cu(II), such as 2-(*N*-morpholino)ethanesulfonic acid (MES) at pH 6.5. The backbone assignment of K32 is complicated by the limited chemical shift dispersions in the proton dimension. Moreover, half of the protein is constituted of five amino acid types only, causing severe resonance overlap. However, the comparison between the $^1H-^{15}N$ HSQC of K32 in phosphate buffer at pH 6.8 and the $^1H-^{15}N$ HSQC of K32 in MES buffer at pH 6.5 showed only a limited number of changes. Therefore, unambiguous assignment of K32 in MES buffer at pH 6.5 could be performed using a three-dimensional HNCA spectrum. The previously determined backbone assignment of K32 in phosphate buffer was used as reference. The Cα resonances of twenty residues were missing in the HNCA spectra of K32 in MES buffer, precluding their sequence-specific assignment.

K32 is disordered in solution, as demonstrated by its hydrodynamic radius (Figure 5B) and $^1H-^{15}N$ HSQC (Figure 2A). However, it has been previously shown that disordered proteins can transiently populate elements of secondary structure (*38*). Circular dichroism (CD) spectra for K32 and K32Δcys were recorded in ammonium acetate buffer (Figure 2B). Typical for disordered polypeptides, the CD spectra showed a strong negative band around 200 nm and an ellipticity around zero at 220 nm. Analysis of the CD spectra using the software CDSSTR, SELCON3 and ContinLL on the DICHROWEB platform (*35*) suggested an average 2.7% of residual helical structure, 3.8% of β-strands, 8.5% turns and 78.7% of unordered structure. No significant differences between the spectra of the two proteins were detectable.

To obtain residue specific information about transient elements of secondary structure, we used NMR chemical shifts (Figure 2C). Cα chemical shifts are very sensitive probes of secondary structure propensities for both globular and unfolded proteins (*34*). The stretches G273−L284, located at the boundary between R1 and R2, S305−L315, which encompass R2 and R3, and Q336−S341, which constitute the boundary between R3 and R4, all showed β-structure propensity. They comprised the two hexapeptides VQIINK and VQIVYK that are important to trigger Tau aggregation into PHFs. A quantitative analysis of the averaged secondary chemical shifts was performed as previously described (*20*). The three stretches were populated 20.3%, 12.7% and 16.7% of time. The regions of β-structure propensity of repeats R2, R3 and R4 are followed by a β-turn as suggested by positive Cα secondary chemical shifts of residues S285, S316 and D348. In addition, residues P223−R230 and P247−L253 in the P2 and R1 region, respectively, had a propensity for extended structure.

Htau40 and K32 Bind One Atom of Cu(II) per Monomer. To determine the Cu(II) binding parameters, an isothermal titration calorimetry experiment (ITC) was performed. In a typical ITC titration experiment (Figure 3A, 3C and 3E), the raw data correspond to the power required by the calorimeter to maintain a constant temperature during and following injection. Each heat pulse corresponds to an injection of ligand into the protein solution. Integration of the exothermic peaks obtained upon copper binding to Tau yields the enthalpy change that follows each injection.

Integrated heat data (Figure 3B and 3D) were fitted using a nonlinear least-squares minimization algorithm. ΔH (reaction enthalpy change in cal mol^{-1}), K_b (binding constant in M^{-1}) and n (number of binding sites) were the fitting

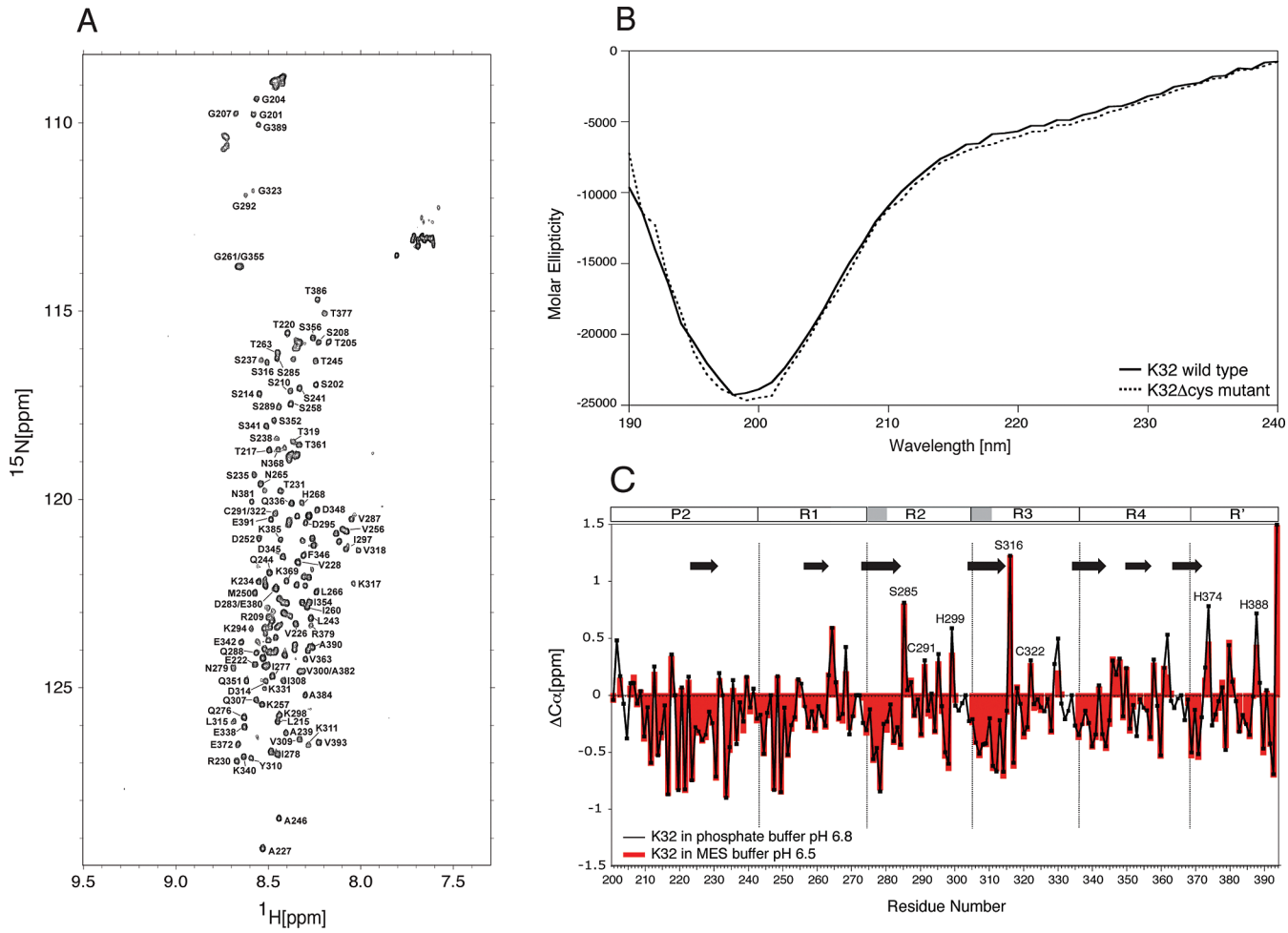

FIGURE 2: Secondary structure propensity of K32 in MES buffer. A. ^{1}H−^{15}N HSQC of K32 in MES buffer at pH 6.5. Resonances are labeled by their residue number. B. CD spectra of K32 (solid line) and K32Δcys (dashed line). C. Cα secondary chemical shifts observed in K32 as a function of residue number. Red bars indicate K32 in MES buffer at pH 6.5 while the black line shows values previously observed in phosphate buffer at pH 6.8. Negative secondary chemical shifts spanning several residues indicate propensity for β-structure (highlighted by arrows). The bar diagram on the top shows the domain organization of K32, while vertical lines indicate domain boundaries. Selected residues are labeled. Gray boxes indicate the two hexapeptides in R2 and R3.

parameters. The reaction entropy was calculated using the relationships $\Delta G = -RT \ln K_b$ ($R = 1.9872$ cal mol^{-1} K^{-1}, $T = 298$ K) and $\Delta G = \Delta H - T\Delta S$. The reduced chi-square parameter χ_v^2 ($\chi_v^2 = \chi^2/n$, where n is the degrees of freedom, $n = N_{idp} - N_{par}$, N_{idp} = number of points, and N_{par} = number of parameters floating in the fit) was used to establish the best fit. For both Htau40 and wild type K32, the best fit was obtained using the one set of sites scheme, with a result of, respectively, 0.912 ± 0.009 and 0.968 ± 0.012 number of binding sites. This indeed indicated that the two proteins bind one copper ion per monomer with a dissociation constant K_d of 0.5 ± 0.1 μM for Htau40 and 0.7 ± 0.1 μM for K32. In the case of K32, the binding process showed a large favorable enthalpic contribute ($\Delta H = -14.6$ kcal mol^{-1}), which compensates the negative entropic factor ($\Delta S = -20.6$ cal mol^{-1} K^{-1}). Htau40 interaction with Cu(II) is also enthalpically driven, but the reaction is less exothermic ($\Delta H = -3.5$ kcal mol^{-1}). The smaller enthalpic factor is balanced by the positive entropy ($\Delta S = 17.2$ cal mol^{-1} K^{-1}). The values given for ΔH and ΔS are apparent and include contributions not only from copper binding but also from associated events such as deprotonation of the cysteines and consequent change in the buffer ionization state.

No interaction, measurable as an enthalpy change, occurred between K32ΔCys and copper under experimental conditions identical to the ones used for the wild type protein (Figure 3F), indicating that the mutated cysteines are essential for metal binding.

Mapping Cu(II) Binding Sites by NMR Spectroscopy. We analyzed the binding of Cu(II) to K32 at residue resolution and monitored protein changes upon metal addition, performing NMR titration experiments on ^{15}N labeled K32 and K32Δcys samples using small (0.5−33%) molar concentration of Cu(II). In the case of wild type K32, the addition of Cu(II) induced chemical shift changes and reduction of signal intensities for a selected set of residues (Figure 4A). Most strongly influenced were the NMR signals of the two peptides ^{287}VQSKCGS^{293} and ^{310}YKPVDLSKVTSKCGS^{324}. Their signal intensities dropped until complete disappearance of the peaks at higher Cu(II) concentrations. In addition, the tetrapeptide ^{306}VQIV^{309} and several histidines (H299, H329, H330, H374, H388) were affected by addition of Cu(II) (Figure 4B). A new set of resonances appeared for V287, ^{309}VYK^{311}, D314 and ^{316}SKVTSK^{321} in the course of the titration (Figure 4C). When the concentration of Cu(II) was further increased, these signals were also broadened. For

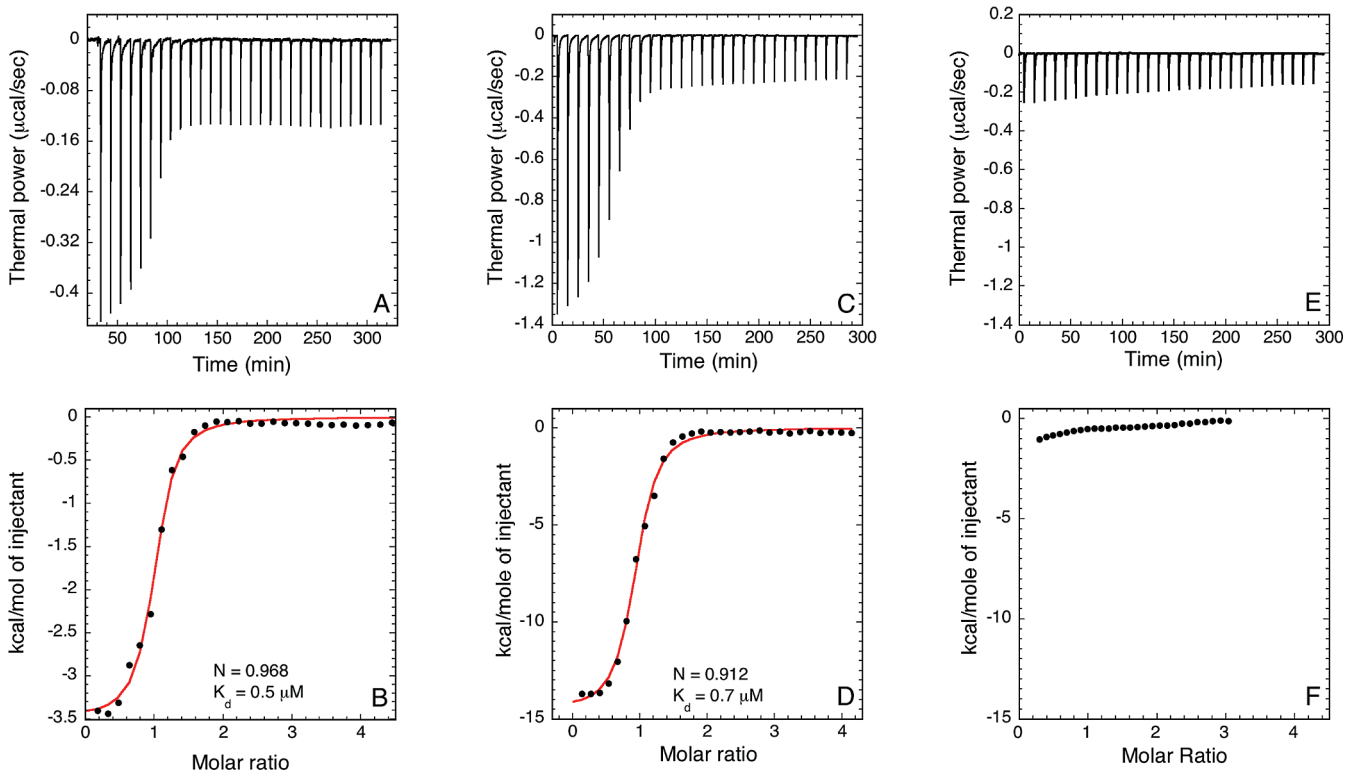

FIGURE 3: Tau:Cu(II) interaction studied by ITC. ITC raw data for titration of Htau40 (A), K32 (C), and K32ΔCys (E) with Cu(II). The integrated heat data (filled circles) are shown in panels B (Htau40), D (K32) and F (K32ΔCys) together with the fit of the data obtained with a single binding site model (red line). The calculated molar ratio *N* of the Cu(II):protein and the dissociation constant are indicated. Experimental conditions as described in the text.

Cu(II):K32 ratios above 0.2, the C-terminal part of the protein comprising the repeat R4 and R′, as well as the second half of R1, showed significant chemical shift changes and signal broadening (data not shown). In the C-terminal part of K32, several negative charged residues are located suggesting unspecific electrostatic interactions at high concentrations of copper. No changes in signal position or intensity were observed for residues M195 to K281, indicating that the N-terminal region is not involved in metal binding.

To test the reversibility of the changes in the NMR spectra, we added a 10-fold excess of EDTA. The signal at the position of the two cysteines, which had been broadened beyond the detection level by addition of copper, appeared again (Figure S4A in the Supporting Information). Thus, at least part of the observed effects is due to a direct binding of Cu(II) to Tau. As the two cysteines have identical $^{1}H/^{15}N$ chemical shifts, we cannot determine if the resonances of both residues were recovered. Moreover, the intensity of the cysteine peak did not reach the value measured in the copper-free state. Upon addition of EDTA, most of the double resonance peaks, except G292, Y310, L315, L376, ^{320}SKGS^{324}, G326 and H329, recovered up to 10% of the original intensity value. The second set of resonances was not present anymore, with the exception of peaks V309, Y310, L315 and K317 (data not shown).

Further addition of DTT, however, completely restored the effects of copper (Figure S4A in the Supporting Information), in analogy with the Fe(III) case (*21*). Therefore the formation of a disulfide bridge due to copper driven oxidation of the two cysteines is likely. SEC-MALS-QELS measurements indicated that any potential disulfide bridge must be intramolecular, as only a single peak distribution corresponding to the monomeric species was found in presence of Cu(II) (Figure S1 in the Supporting Information). A limited oxidation of cysteines was confirmed by the Ellman's assay (Figure S4C in the Supporting Information). In the presence of an equal molar amount of Cu(II), the concentration of free sulfhydryls showed a 10% reduction. The phenomenon was concentration dependent, and a 10-fold excess of copper resulted in a lower percentage of −SH reactive groups available (Figure S4C in the Supporting Information).

To further confirm the ITC results, a NMR titration experiment was also performed on K32Δcys (Figure S3 in the Supporting Information). In clear contrast to wild type K32, NMR signals remained unaffected up to a Cu(II):K32Δcys ratio of 0.03 (Figure S3A,D in the Supporting Information), whereas at higher Cu(II):K32Δcys ratios unspecific binding of Cu(II) to the C-terminal domain of K32Δcys was observed (Figure S3B,C,E,F in the Supporting Information). In particular, no drop in signal intensity was observed for the two peptides ^{287}VQSKCGS^{293} and ^{310}YKPVDLSKVTSKCGS^{324}. Thus, the cysteine residues are essential for binding of Tau to copper, in agreement with the ITC data. Preliminary studies on a 99-residue Tau fragment containing only repeats one, three and four (K19) showed that Tau isoforms containing only three repeats are also able to bind to Cu(II) (data not shown).

K32 Remains Disordered in the Presence of Cu(II). We studied the secondary structure of K32 in the presence of Cu(II). CD spectra of K32 in the free state and in the presence of Cu(II) were highly similar (data not shown), indicating that K32 remained mainly disordered. This was supported by NMR secondary chemical shifts. Upon addition of 5% of copper sulfate, hardly any changes in Cα secondary

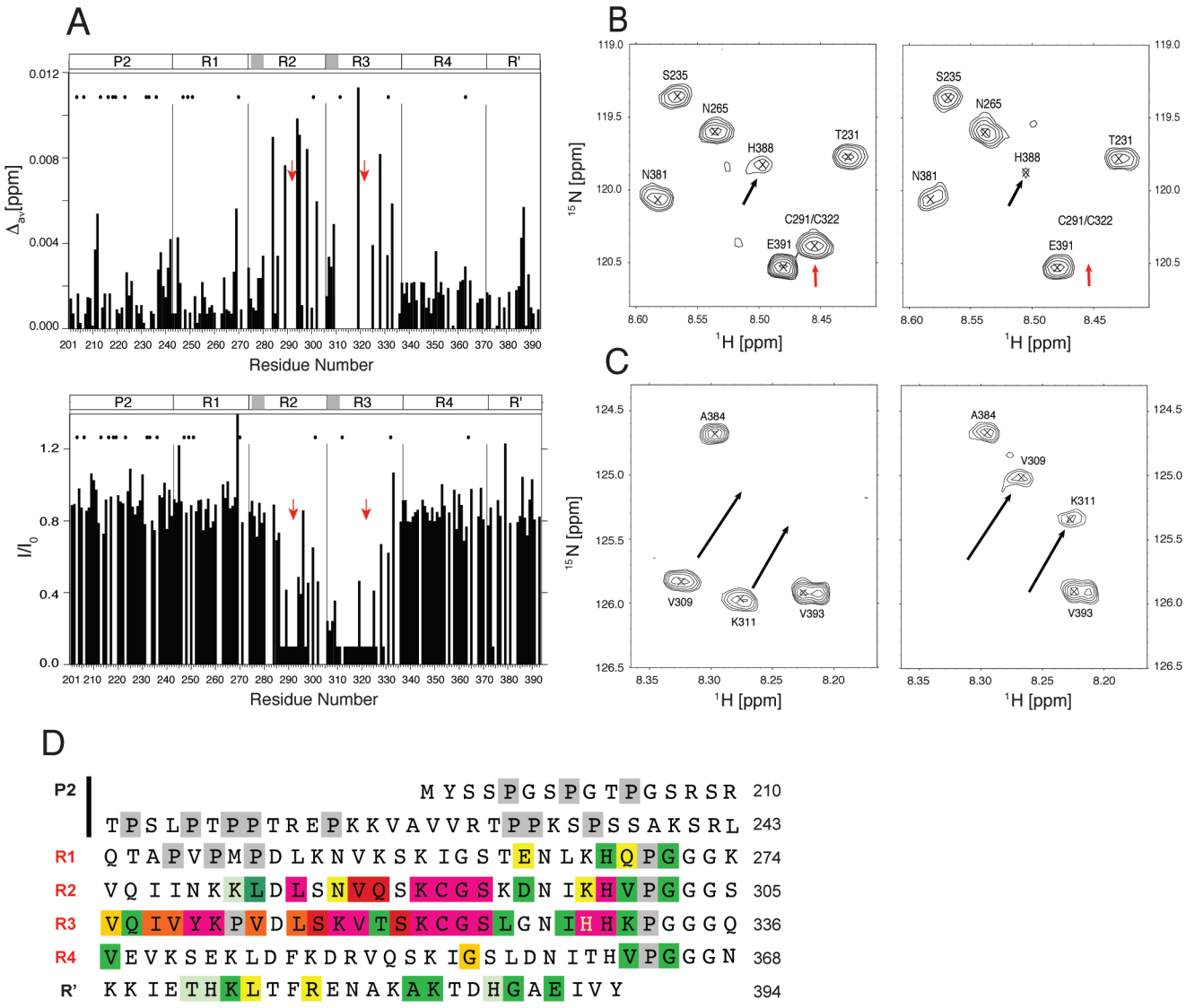

FIGURE 4: Mapping the K32:Cu(II) binding site at single residue resolution. A. Averaged and weighted chemical shift change for each backbone amide group in K32 upon addition of Cu(II) (upper panel). Intensity profiles of the corresponding titration step (Cu(II):K32 ratio of 0.2) are shown below. Peaks that disappeared were scaled to 0.1 for the purpose of clarity. Repeat boundaries are marked by vertical dashed lines. Gaps are due to proline (black dots) or overlapping peaks. The position of the two cysteines is indicated by arrows. B. Selected region of the ^{1}H−^{15}N HSQC in the absence of copper (left) and for a Cu(II):K32 ratio of 0.1 (right). The signals of the two cysteines overlap (red arrow). C. Selected region of the ^{1}H−^{15}N HSQC highlighting the appearance of new resonances for the residues V309 and K311 upon addition of copper (right; Cu(II):K32 ratio of 0.05). On the left, the same region in the absence of copper is shown. The direction of the signal shifts is indicated by arrows. D. Summary of residues of K32 affected by addition of Cu(II). Strongly broadened residues are shown in red. Decreased broadening is indicated by pink, orange, yellow and green (only broadened at high copper concentrations). Prolines are depicted in gray.

chemical shifts were observed (Figure 5A). However at intermediate concentrations of copper, a second set of resonances was observed for residues located in the binding site (see above), suggesting the presence of a Cu(II) bound conformation of K32 that differs from the free state. Unfortunately, the involved resonances (V287, ^{309}VYK^{311}, D314 and ^{316}SKVTSK^{321}) could not be detected in HNCA or HNCO spectra excluding a characterization of their secondary structure propensity. Further support for Cu(II)-induced conformational changes came from the measurement of the diffusion properties of K32 in the presence of copper (Figure 5B). The hydrodynamic radii calculated from the DOSY diffusion data using aliphatic resonances were 4.5 nm in the free state and 3.0 nm when Cu(II) was bound to K32.

K32 Shows Limited Cu(II)-Induced Aggregation. We measured dynamic light scattering (DLS) on apo K32 and K32:Cu(II) to analyze the possibility of a copper-driven aggregation. We could follow the appearance of a peak around 100−150 nm of diameter upon addition of copper (Figure 6). The intensity of the peak increased in subsequent steps of the titration. However, the total concentration of aggregates was below 1%. For this reason, it was not possible to detect the species with other techniques. Addition of EDTA to the reaction reversed the effect of copper on aggregation (Figure S4B in the Supporting Information).

DISCUSSION

Monomeric Tau in solution is an intrinsically disordered protein that lacks a rigid secondary or tertiary structure (*18*). We previously characterized at single-residue resolution the structural propensities of a 198-residue fragment of Tau

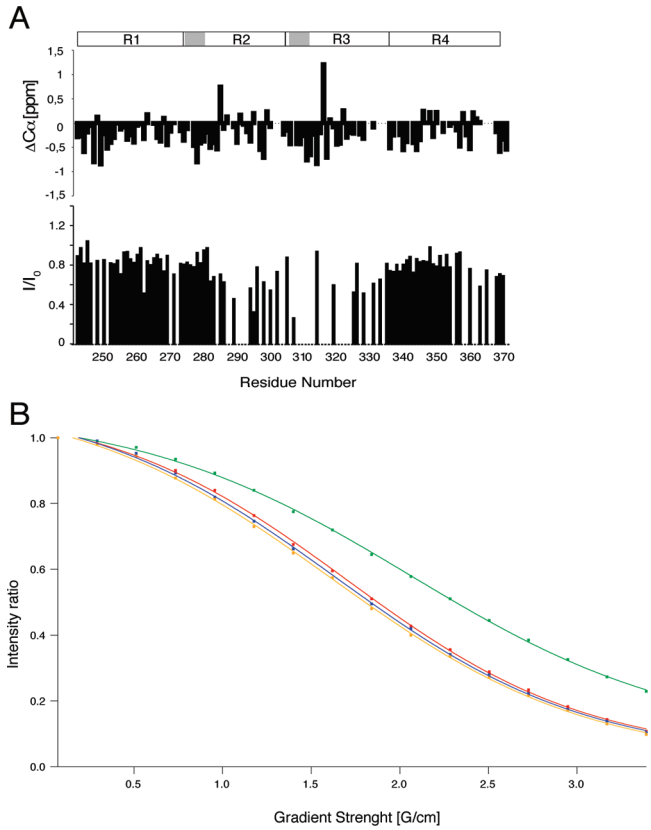

FIGURE 5: Cu(II)-induced structural changes in K32. A. Cα secondary chemical shifts of the repeat region of Tau in the presence of Cu(II) at a ratio of 0.05 (top panel). The intensity reduction profile at the same Cu(II) concentration is shown below. B. Diffusion properties of K32. Intensity decay of methyl signals of K32 for increasing gradient strengths in the absence of Cu(II) (green) and at Cu(II) ratios of 0.03 (red), 0.1 (blue) and 0.6 (yellow), respectively.

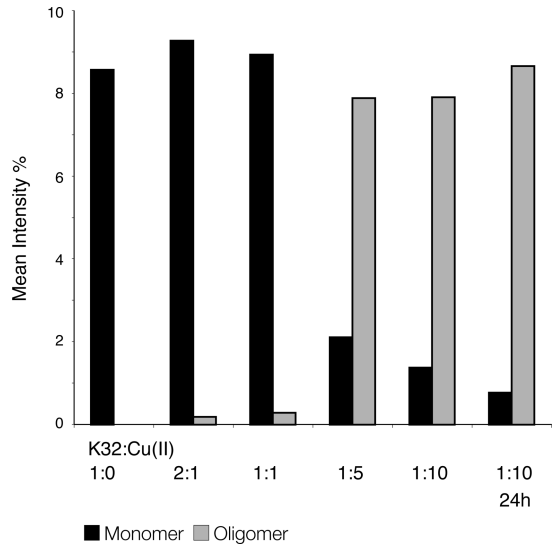

FIGURE 6: Cu(II) induces a limited amount of oligomerization of K32. Mean scattering intensities of the monomeric (black) and oligomeric peak (gray) observed by DLS. In the absence of copper (titration point 1), only a peak at 4.5 nm was observed corresponding to monomeric K32. Titration points 2 to 6 correspond to K32:Cu(II) ratios of 2:1, 1:1, 1:5, 1:10 and 1:10 after 24 h. The Cu(II)-induced oligomers had a diameter of 100−150 nm.

(K32) that comprises the four repeat motifs and the two flanking basic domains P2 and R′ (*20*). These previous studies were performed in phosphate buffer at pH 6.8. To enable interaction studies with Cu(II), a different buffer was required, namely, MES buffer at pH 6.5. The line width and limited chemical shift dispersion of signals observed in a $^{1}H-^{15}N$ HSQC spectrum of K32 in MES buffer demonstrated that Tau remained highly flexible in these conditions (Figure 2A). In addition, hydrodynamic radius values obtained from NMR diffusion measurements were in full agreement with values expected for a random coil polypeptide comprising 198 residues (Figure 5B). Very similar HSQC and CD patterns were observed for wild type K32 and the K32 mutant, in which cysteine 291 and 322 were replaced by alanines (Figure 2B). Differences in the HSQCs were mostly restricted to residues in the direct vicinity of the sites of mutation (Figure S2B in the Supporting Information).

Sequence specific assignment of the NMR signals of K32 is challenging, due to the small chemical shift dispersion, the repetitive nature of the pseudorepeat domain and the large number of prolines in domain P2. Based on the assignment previously obtained in phosphate buffer (*20*), we were able to assign 90% of the backbone chemical shifts of nonproline residues of K32 in MES buffer at pH 6.5. Cα secondary chemical shifts revealed five stretches in K32 that transiently populate β-structure and which are located in the flanking region P2 and in the boundary between P2−R1, R1−R2 and R2−R3. The results are in good agreement with the Cα secondary chemical shifts observed for the same protein in phosphate buffer at pH 6.8, indicating that the different buffer and pH have negligible effects on the structural propensities of K32 in solution (Figure 2C).

Binding of Cu(II) to Tau was initially characterized by ITC. The technique allows the estimation of the number of binding sites and of the affinity of the binding reaction. Our data indicate that Htau40 and K32 are able to bind one Cu(II) ion per molecule (Figure 3). With K_d values of 0.5 μM and 0.7 μM, respectively, the affinities of Cu(II) for Htau40 and K32 were very similar, suggesting that K32 comprises the copper ion binding site. This information, together with previous data on fibrillization behavior, MT and heparin binding, enforces the role of K32 as model peptide for Tau studies in vitro. ITC could not detect any binding of Cu(II) to K32Δcys under identical experimental conditions, indicating that the two cysteines present in four-repeat Tau (C291 and C322) are essential for the interaction. Noteworthy, the affinities observed for the Tau:Cu(II) interaction are comparable to values measured previously for other disordered proteins involved in neurodegenerative disease, such as α-synuclein (∼0.1 μM) (*12*), SHaPrP(23−231) (∼14 μM at pH 6) (*39*) or Aβ_{40} (∼30 μM at pH 7.4) (*11*).

To map the copper-binding site at single residue resolution, we employed NMR chemical shift perturbation analysis. In addition, NMR signal intensities are a very sensitive probe for the interaction, as Cu(II) is a paramagnetic metal that broadens NMR signals directly bound to it. These tools demonstrated that the binding site of Cu(II) to K32 is mainly located in repeats R2 and R3 (Figure 4A and 4D). In particular, the two polypeptides ^{287}VQSKCGS^{293} and ^{310}YKPVDLSKVTSKCGS^{324}, and to a smaller degree ^{306}VQIV^{309}, are strongly influenced by addition of copper. Moreover, histidines 299 (in R2), 329 and 330 (in R3) contribute to the interaction (Figure 4D). This is in agreement with previous studies on short peptides comprising either repeat

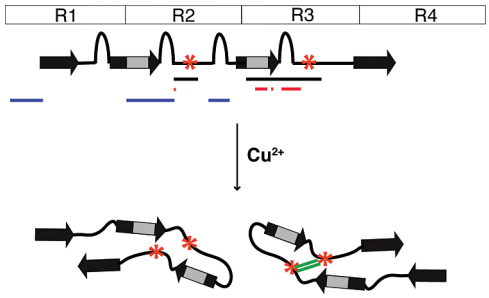

FIGURE 7: Schematic diagram illustrating the effect of Cu(II) binding on the structure of the repeat region of Tau. Elements of transient β-structure observed in K32 using NMR secondary chemical shifts are shown as arrows. Turns and disordered regions are drawn as curved and straight lines, respectively. The positions of the cysteines are marked by red stars, the two hexapeptides (275−280, 306−311) by gray boxes. Black lines mark the copper binding site (see text), while red lines highlight those residues for which new resonances appeared in the presence of Cu(II). Blue lines show the MT binding sites. Upon addition of copper, R2 and R3 come into spatial proximity leading to a compaction of K32. An intramolecular disulfide bridge due to metal-driven cysteines oxidation can occur.

R2 or repeat R3 (*25, 26*). Our data suggest that R1 does not contribute to the binding as much as R2 and R3, in contrast to Zhou et al. (*24*). Moreover, as indicated by our ITC measurements, only one Cu(II) ion binds to one Tau molecule. This suggests that the metal ion binds simultaneously to the two peptides R2 and R3, bringing reacting groups from the two repeats close together (Figure 7). In contrast, microtubules primarily interact with residues not involved in the Cu(II) binding: ^{225}KVAVVRT^{231},^{240}KSRLQTAPV^{248}, ^{275}VQIINKKLDLS^{285}, ^{297}IKHV^{300}, ^{370}KIETHKLTFREN^{381} (Figure 7), suggesting that copper can also bind to MT-bound Tau thus affecting most of the Tau molecules in the cell.

The requirement of cysteines for the interaction raises the possibility of the formation of a disulfide bridge. MALS did not detect any low molecular weight aggregates in the presence of Cu(II), indicating that intermolecular disulfide bridge formation does not play a significant role. To evaluate the formation of an intramolecular disulfide bridge, we added EDTA and DTT to the NMR sample containing Cu(II). Addition of EDTA only partially restored the intensity of the cross peaks of the two cysteines. Only in the presence of a reducing agent, such as DTT, the effect of Cu(II) was completely reversed. This suggests that part of the observed effects might be due to formation of an intramolecular disulfide bridge in the presence of the oxidizing copper ion, as confirmed by the reduction of the concentration of free thiol in solution upon incubation with Cu(II) (Figure S4C in the Supporting Information).

To further investigate the role of the cysteines, we performed experiments on the interaction of Cu(II) with a fragment of three-repeat Tau. This 99-residue fragment named K19 contains only repeats R1, R3 and R4, while R2 is not present. ITC showed that Cu(II) is able to bind to K19 (data not shown), indicating that the presence of C322 is sufficient for binding. However, the affinity of the interaction differed from that observed for K32. Although these are preliminary observations, they underline that formation of an intramolecular disulfide bridge is not essential for Tau:Cu(II) interaction, but can be a consequence of the metal binding. Moreover, Li et al., recently found that R2 can get oxidized into stable disulfide-linked dimers in presence of Cu(II) (*40*). In analogy, metal catalyzed oxidation has been reported for other copper binding proteins, including SHaPRP(29−231) (*41*), and is likely to target residues with metal binding affinity, such as histidines or cysteines.

Cα secondary chemical shifts in the absence and presence of copper were very similar, suggesting that binding of Cu(II) does not induce structural changes (Figure 5A). However, the analysis is complicated by the fact that signals directly bound to Cu(II) are broadened beyond detection. Thus, only at low concentrations of Cu(II) the NMR signals of the interacting residues are observed at which most of the protein molecules remain in the unbound state. Nevertheless, several elements point to a conformational change induced by binding to Cu(II). A second set of resonances appeared for residues V287, ^{309}VYK^{311}, D314 and ^{316}SKVTSK^{321} in the presence of Cu(II) (Figure 4C). However, as these signals were very weak, the corresponding Cα resonances could not be detected in an HNCA spectrum excluding their further characterization. Interestingly, some of these residues are part of the ^{306}VQIVYKPVD^{314} hexapeptide in R3 that is essential for aggregation of Tau into PHFs (*17*). Further support for a structural change came from NMR diffusion measurements: upon addition of Cu(II) a reduction in the hydrodynamic radius of K32 was observed (Figure 5B). An overall compaction of the ensemble of structures populated by K32 in solution is in agreement with the fact that binding of Cu(II) brings residues in repeats R2 and R3 in spatial proximity to form the binding site. This effect might be partially due to the formation of the intramolecular disulfide bridge. Noteworthy, no compaction was observed for α-synuclein in the presence of Cu(II) (*10*).

There is increasing evidence that prefibrillar species can be toxic, often even more than their fibrillar counterparts (*42*). Using light scattering, we showed that Cu(II) induces a small amount of amorphous aggregates, less than 1% (Figure 6). The aggregates are brought about by a direct Cu(II) effect, as far as the addition of EDTA partially reverses the aggregation (Figure S4B in the Supporting Information). However, it is difficult to characterize these species at higher resolution due to their low concentration, their presumably heterogeneous nature, and their large molecular weight. In addition, further studies are required to probe any potential role of these aggregates in the pathway of Tau misfolding and neurotoxicity.

Copper can promote the formation of aggregates and amyloid fibrils of a number of proteins (*11, 41, 43*). The interaction studies reported here were performed at close to physiological conditions (∼100 mM NaCl). These conditions (i.e., high ionic strength) are not suitable for *in vitro* aggregation experiments of Htau40 or its fragments, due to a greatly reduced rate of aggregation. To induce aggregation of Tau or its fragments in these conditions, the addition of polyanions (heparin) is required, which overrules the effect of copper. Moreover, aggregation of 4-repeat Tau is strongly attenuated in the absence of a reducing agent due to the formation of intramolecular disulfide bridges (*44*). However, addition of DTT to the *in vitro* aggregation assay is not possible as it prevents the effect of copper. As discussed above we observed binding of Cu(II) to Tau followed by oxidation of cysteines. This suggests that in the presence of

copper the rate of aggregation of 4-repeat Tau is reduced, whereas it is increased in 3-repeat Tau due to the formation of intermolecular disulfide bridges. Notably, it was previously shown that aluminum and iron only enhanced Tau aggregation when the protein was hyperphosphorylated (*22, 23*).

ACKNOWLEDGMENT

We thank Lukasz Skora, Min-Kyu Cho and Dr. Vinesh Vijayan for the help with NMR measurements. The MicroCal VP-ITC instrument is part of the Consorzio Interdipartimentale Ricerche in Biotecnologie (CIRB) of the University of Bologna.

SUPPORTING INFORMATION AVAILABLE

SEC-MALS analysis of K32 apo and Cu(II) bound, NMR properties of K32Δcys, chemical shift changes and intensity ratios of K32Δcys in presence of copper, EDTA effect on Cu(II) binding to K32, quantification of metal oxidized cysteines and Cα secondary chemical shifts in presence of Cu(II). This material is available free of charge via the Internet at http://pubs.acs.org.

REFERENCES

1. Ferri, C. P., Prince, M., Brayne, C., Brodaty, H., Fratiglioni, L., Ganguli, M., Hall, K., Hasegawa, K., Hendrie, H., Huang, Y. Q., Jorm, A., Mathers, C., Menezes, P. R., Rimmer, E., and Scazufca, M. (2005) Global prevalence of dementia: a Delphi consensus study. *Lancet 366*, 2112–2117.
2. Kukull, W. A., Higdon, R., Bowen, J. D., McCormick, W. C., Teri, L., Schellenberg, G. D., van Belle, G., Jolley, L., and Larson, E. B. (2002) Dementia and Alzheimer disease incidence - A prospective cohort study. *Arch. Neurol. 59*, 1737–1746.
3. Lindsay, J., Laurin, D., Verreault, R., Hébert, R., Helliwell, B., Hill, G. B., and McDowell, I. (2002) Risk Factors for Alzheimer's Disease: A Prospective Analysis from the Canadian Study of Health and Aging. *Am. J. Epidemiol. 156*, 445–453.
4. Perry, G., Sayre, L. M., Atwood, C. S., Castellani, R. J., Cash, A. D., Rottkamp, C. A., and Smith, M. A. (2002) The role of iron and copper in the aetiology of neurodegenerative disorders - Therapeutic implications. *CNS Drugs 16*, 339–352.
5. Barnham, K. J., McKinstry, W. J., Multhaup, G., Galatis, D., Morton, C. J., Curtain, C. C., Williamson, N. A., White, A. R., Hinds, M. G., Norton, R. S., Beyreuther, K., Masters, C. L., Parker, M. W., and Cappai, R. (2003) Structure of the Alzheimer's disease amyloid precursor protein copper binding domain - A regulator of neuronal copper homeostasis. *J. Biol. Chem. 278*, 17401–17407.
6. Miura, T., Suzuki, K., Kohata, N., and Takeuchi, H. (2000) Metal binding modes of Alzheimer's amyloid beta-peptide in insoluble aggregates and soluble complexes. *Biochemistry 39*, 7024–7031.
7. Strausak, D., Mercer, J. F. B., Dieter, H. H., Stremmel, W., and Multhaup, G. (2001) Copper in disorders with neurological symptoms: Alzheimer's, Menkes and Wilson disease. *Brain Res. Bull. 55* (2), 175–185.
8. Sayre, L. M., Perry, G., Harris, P. L. R., Liu, Y., Schubert, K. A., and Smith, M. A. (2000) In situ oxidative catalysis of Neurofibrillary Tangles and Senile Plaques in Alzheimer's Disease: A central role for bound transition metals. *J. Neurochem. 74* (1), 270–279.
9. Rae, T. D., Schmidt, P. J., Pufahl, R. A., Culotta, V. C., and O'Halloran, T. V. (1999) Undetectable intracellular free copper: the requirement of a copper chaperon for superoxide dismutase. *Science 284*, 805–808.
10. Perry, G., Taddeo, M. A., Petersen, R. B., Castellani, R. J., Harris, P. L. R., Siedlak, S. L., Cash, A. D., Liu, Q., Nunomura, A., Atwood, C. S., and Smith, M. A. (2003) Adventiously-bound redox active iron and copper are at the center of oxidative damage in Alzheimer disease. *BioMetals 16*, 77–81.
11. Tõugu, V., Karafin, A., and Palumaa, P. (2008) Binding of zinc(II) and copper(II) to the full-length Alzheimer's amyloid-β peptide. *J. Neurochem. 104* (5), 1249–1259.
12. Rasia, R. M., Bertoncini, C. W., Marsh, D., Hoyer, W., Cherny, D., Zweckstetter, M., Griesinger, C., Jovin, T. M., and Fernandez, C. O. (2005) Structural characterization of copper(II) binding to alpha-synuclein: Insights into the bioinorganic chemistry of Parkinson's disease. *Proc. Natl. Acad. Sci. U.S.A. 102*, 4294–4299.
13. Millhauser, G. L. (2007) Copper and the prion protein: methods, structures, function, and disease. *Annu. Rev. Phys. Chem. 58*, 299–320.
14. Buee, L., Hamdane, M., Delobel, P., Bussiere, T., Sergeant, N., and Delacourte, A. (2002) Role of Tau in Alzheimer's disease and other tauopathies. *Mov. Disord. 17*, 1407–1407.
15. Schneider, A., Biernat, J., von Bergen, M., Mandelkow, E., and Mandelkow, E. M. (1999) Phosphorylation that detaches Tau from microtubules S262 and S214 protects it against aggregation into Alzheimer paired helical filaments. *J. Neurochem. 73*, S26−S26.
16. Braak, H., and Braak, E. (1991) Neuropathological staging of Alzheimer-related changes. *Acta Neuropathol. 82*, 239–259.
17. von Bergen, M., Friedhoff, P., Biernat, J., Heberle, J., Mandelkow, E. M., and Mandelkow, E. (2000) Assembly of Tau protein into Alzheimer paired helical filaments depends on a local sequence motif (306-VQIVYK-311) forming beta structure. *Proc. Natl. Acad. Sci. U.S.A. 97* (10), 5129–5134.
18. Schweers, O., Schonbrunnhanebeck, E., Marx, A., and Mandelkow, E. (1994) Structural studies of tau-protein and Alzheimer paired helical filaments show no evidence for beta-structure. *J. Biol. Chem. 269*, 24290–24297.
19. Dyson, J. H., and Wright, P. E. (1998) Equilibrium NMR studies of unfolded and partially folded proteins. *Nat. Struct. Mol. Biol. 5*, 499–503.
20. Mukrasch, M. D., von Bergen, M., Biernat, J., Fischer, D., Griesinger, C., Mandelkow, E., and Zweckstetter, M. (2007) The "jaws" of the Tau-microtubule interaction. *J. Biol. Chem. 282*, 12230–12239.
21. Cappai, R., Cheng, F., Ciccotosto, G. D., Needham, B. E., Masters, C. L., Multhaup, G., Fransson, L. A., and Mani, K. (2007) The amyloid precursor protein (APP) of Alzheimer disease and its paralog, APLP2, modulate the Cu/Zn-Nitric Oxide-catalyzed degradation of glypican-1 heparan sulfate in vivo. *J. Biol. Chem. 280* (14), 13913–13920.
22. Shin, R. W., Lee, V. M. Y., and Trojanowski, J. Q. (1994) Aluminium modifies the properties of Alzheimers-disease PHF-tau proteins in vivo and in vitro. *J. Neurosci. 14*, 7221–7233.
23. Yamamoto, A., Shin, R. W., Hasegawa, K., Naiki, H., Sato, H., Yoshimasu, F., and Kitamoto, T. (2002) Iron (III) induces aggregation of hyperphosphorylated Tau and its reduction to iron (II) reverses the aggregation: implications in the formation of neurofibrillary tangles of Alzheimer's disease. *J. Neurochem. 82*, 1137–1147.
24. Zhou, L. X., Du, J. T., Zeng, Z. Y., Wu, W. H., Zhao, Y. F., Kanazawa, K., Ishizuka, Y., Nemoto, T., Nakanishi, H., and Li, Y. M. (2007) Copper (II) modulates in vitro aggregation of a Tau peptide. *Peptides 28* (11), 2229–2234.
25. Ma, Q. F., Li, Y. M., Du, J. T., Liu, H. D., Kanazawa, K., Nemoto, T., Nakanishi, H., and Zhao, Y. F. (2006) Copper binding properties of a Tau peptide associated with Alzheimer's disease studied by CD, NMR, and MALDI-TOF MS. *Peptides 27*, 841–849.
26. Ma, O. F., Li, Y. M., Du, J. T., Kanazawa, K., Nemoto, T., Nakanishi, H., and Zhao, Y. F. (2005) Binding of copper (II) ion to an Alzheimer's Tau peptide as revealed by MALDI-TOF MS, CD, and NMR. *Biopolymers 79*, 74–85.
27. Atwood, C. S., Moir, R. D., Huang, X. D., Scarpa, R. C., Bacarra, N. M. E., Romano, D. M., Hartshorn, M. K., Tanzi, R. E., and Bush, A. I. (1998) Dramatic aggregation of Alzheimer A beta by Cu(II) is induced by conditions representing physiological acidosis. *J. Biol. Chem. 273*, 12817–12826.
28. Barghorn, S., Biernat, J., and Mandelkow, E. (2005) *Methods Mol. Biol. (Clifton, NJ) 299*, 35–51.
29. Yamazaki, T., Lee, W., Revington, M., Mattiello, D. L., Dahlquist, F. W., Arrowsmith, C. H., and Kay, L. E. (1994) An HNCA pulse scheme for the backbone assignment of ^{15}N,^{13}C,^{2}H-labeled proteins: application to a 37-kDa *Trp* repressor−DNA complex. *J. Am. Chem. Soc. 116*, 6464–6465.
30. Markley, J. L., Bax, A., Arata, Y., Hilbers, C. W., Kaptein, R., Sykes, B. D., Wright, P. E., and Wuthrich, K. (1998) Recommendations for the presentation of NMR structures of proteins and nucleic acids - IUPAC-IUBMB-IUPAB inter-union task group on the standardization of data bases of protein and nucleic acid structures determined by NMR spectroscopy. *Eur. J. Biochem. 256*, 1–15.

31. Delaglio, F., Grzesiek, S., Vuister, G. W., Zhu, G., Pfeifer, J., and Bax, A. (1995) NMRPipe - a multidimensional spectral processing system based on Unix pipes. *J. Biomol. NMR 6*, 277–293.
32. Goddard, T. D., and Kneller, D. G., *SPARKY 3*, University of California, San Francisco.
33. Wilkins, D. K., Grimshaw, S. B., Receveur, V., Dobson, C. M., Jones, J. A., and Smith, L. J. (1999) Hydrodynamic radii of native and denatured proteins measured by pulse field gradient NMR techniques. *Biochemistry 38*, 16424–16431.
34. Wishart, D. S., and Sykes, B. D. (1994) The C-13 chemical-shift index - a simple method for the identification of protein secondary structure using C-13 chemical-shift data. *J. Biomol. NMR 4*, 171–180.
35. Lobley, A., Whitmore, L., and Wallace, B. A. (2002) DICHROWEB: an interactive website for the analysis of protein secondary structure from circular dichroism spectra. *Bioinformatics 18*, 211–212.
36. Stola, M., Musiani, F., Mangani, S., Turano, P., Safarov, N., Zambelli, B., and Ciurli, S. (2006) The nickel site of Bacillus pasteurii UreE, a urease metallo-chaperone, as revealed by metal-binding studies and X-ray absorption spectroscopy. *Biochemistry, 45*, 6495–6509.
37. Cleveland, D. W., Hwo, S. Y., and Kirschner, M. W. (1977) Physical and chemical properties of purified tau factor and role of tau in microtubule assembly. *J. Mol. Biol. 116*, 227–247.
38. Fink, A. L. (2005) Natively unfolded proteins. *Curr. Opin. Struct. Biol. 15*, 35–41.
39. Stöckel, J., Safar, J., Wallace, A. C., Cohen, F. E., and Prusiner, S. B. (1998) Prion protein selectively binds copper(II) ions. *Biochemistry 37*, 7185–7193.
40. Su, X. Y., Wu, W. H., Huang, Z. P., Hu, J., Lei, P., Yu, C. H., Zhao, Y. F., and Li, Y. M. (2007) Hydrogen peroxide can be generated by tau in the presence of Cu(II). *Biochem. Biophys. Res. Commun. 358*, 661–665.
41. Requena, J. R., Groth, D., Legname, G., Stadtman, E. R., Prusiner, S. B., and Levine, R. L. (2001) Copper-catalyzed oxidation of the recombinant SHa(29−231) prion protein. *Proc. Natl. Acad. Sci. U.S.A. 98* (13), 7170–7175.
42. Baglioni, S., Casamenti, F., Bucciantini, M., Luheshi, L. M., Taddei, N., Chiti, F., Dobson, C. M., and Stefani, M. (2006) Prefibrillar amyloid aggregates could be generic toxins in higher organisms. *J. Neurosci. 26*, 8160–8167.
43. Binolfi, A., Rasia, R. M., Bertoncini, C. W., Ceolin, M., Zweckstetter, M., Griesinger, C., Jovin, T. M., and Fernandez, C. O. (2006) Interaction of alpha-synuclein with divalent metal ions reveals key differences: A link between structure, binding specificity and fibrillation enhancement. *J. Am. Chem. Soc. 128*, 9893–9901.
44. Schweers, O., Mandelkow, E. M., Biernat, J., and Mandelkow, E. (1995) Oxidation of cysteine-322 in the repeat domain of microtubule-associated protein tau controls the in vitro assembly of paired helical filaments. *Proc. Natl. Acad. Sci. U.S.A. 92* (18), 8463–8467.

BI8008856